Jinghua, Xu et al.

Article

Energy and exergy co-optimization of IGCC with lower emissions based on fuzzy supervisory predictive control

Energy Reports

Provided in Cooperation with:
Elsevier

Suggested Citation: Jinghua, Xu et al. (2020) : Energy and exergy co-optimization of IGCC with lower emissions based on fuzzy supervisory predictive control, Energy Reports, ISSN 2352-4847, Elsevier, Amsterdam, Vol. 6, pp. 272-285, https://doi.org/10.1016/j.egyr.2020.01.003

This Version is available at:
https://hdl.handle.net/10419/244030

Energy Reports 6 (2020) 272–285

Contents lists available at ScienceDirect

Energy Reports

journal homepage: www.elsevier.com/locate/egyr

Research paper

Energy and exergy co-optimization of IGCC with lower emissions based on fuzzy supervisory predictive control

Xu Jinghua [a,b,c], Wang Tiantian [c], Gao Mingyu [c], Peng Tao [d], Zhang Shuyou [a,b,c,*], Tan Jianrong [a,b,c]

[a] State Key Lab of Fluid Power and Mechatronic Systems, Zhejiang University, Hangzhou 310027, China
[b] Key Lab of Advanced Manufacturing Technology of Zhejiang Province, Hangzhou 310027, China
[c] School of Mechanical Engineering, Zhejiang University, Hangzhou 310027, China
[d] Hangzhou Turbine Machinery Equipment CO., LTD, Hangzhou 310022, China

ARTICLE INFO

Article history:
Received 15 August 2019
Received in revised form 28 November 2019
Accepted 8 January 2020
Available online 23 January 2020

Keywords:
Integrated gasification combined cycle (IGCC)
Energy and exergy co-optimization
Cryogenic air separation unit (ASU)
CO_2 capture and storage unit (CCS)
Heat recovery steam generator (HRSG)
Waste water recovery (WWR)
Fuzzy Supervisory Predictive Control (FSPC)

ABSTRACT

This paper presents an energy and exergy co-optimization method of integrated gasification combined cycle (IGCC) based on Fuzzy Supervisory Predictive Control (FSPC). Firstly, a green IGCC process is proposed which contains three principle couplings: air separation unit (ASU), heat recovery steam generator (HRSG) and CO_2 capture/storage unit (CCS). From law of thermodynamics, using substance thermophysical parameters, the energy efficiency and exergy efficiency of IGCC are successively defined. The IGCC power station has features such as closed coupling, large time lag and non-linearity, however, faster response speed and lower overshoot are always the unremitting pursuits. Therefore, the Fuzzy Supervisory Predictive Control (FSPC) method is proposed to implement robust control under complex disturbances by pre-considering unmeasurable disturbance and measurable disturbance. The fuzzy rules extracted from historical bigdata are employed in supervisory layer to make the precise control decisions. Finally, the energy and exergy co-optimization model is built and solved for higher efficiency and economic effectiveness. Taking the large-scale (300MW) IGCC for example, after using FSPC, the efficiency of water recovery is increased from 40.7% to 62.1% with the ratio of 52.6% because of waste water recovery (WWR) system. The net efficiency of proposed IGCC system is increased from 37.6% to 41.7% with the ratio of 10.9%. The exergy efficiency of IGCC system is increased from 36.5% to 39.2% with the ratio of 7.4%. The proposed method has great significance for the energy-saving and Near-zero emissions (NZEC) IGCC with high safety and robust control under supercritical (SC) or ultra-super critical (USC) state.

1. Introduction

Energy efficiency has become an effective way for sustainable development in the future. Improving the efficiency of energy utilization can significantly improve the quality of energy utilization and reduce energy consumption. Nowadays, the integrated gasification combined cycle (IGCC) is a promising technology for power generation that allows various feedstocks with high efficiency and low greenhouse gas emissions (Chen et al., 2018; Emun et al., 2010; Lee et al., 2014). Coal, biomass or any other suitable solid or liquid feedstocks can be converted to syngas in a gasifier and fed into other subsystems. With the increasingly serious environmental problems, China has issued ultra-low emission standards to limit the carbon dioxide, sulfur dioxide and other polluting gases in large factories (Tang et al., 2019). It is a trend to develop green factory production mode. A typical IGCC system is mainly composed of cryogenic air separation unit (ASU), gasification unit, gas turbine (GT), steam turbine (ST), heat recovery steam generator (HRSG) (Khan and Tlili, 2018), CO_2 capture and storage unit (CCS) and so on. It can also be divided into gasification subsystem, cleaning subsystem, power generation subsystem and waste heat recovery subsystem. The net efficiency of an IGCC system further decreases to 32.5% when considers CCS (Jones et al., 2011). Therefore, improving the efficiency of IGCC system is an urgent requirement. In order to improve the efficiency of IGCC system and reduce its energy requirement, it can be summarized into four approaches according to previous research.

The first approach is to integrate cryogenic ASU with IGCC system by oxygen and nitrogen produced in ASU. The mixture of oxygen and steam is used as the gasification agent instead of the traditional air which can produce syngas with a higher heating value (HHV) greater than 11.11 MJ/N m^3 (Zang et al., 2018). Nitrogen injection in combustor can reduce NOx formation

* Corresponding author.
E-mail address: zsy@zju.edu.cn (GN02Zhang S.).

https://doi.org/10.1016/j.egyr.2020.01.003

in GT and increase turbine power output. The most effective way to produce large quantities of high purity oxygen and nitrogen is cryogenic ASU. The optimization and integration of ASU and GT in IGCC system is very important. Jones et al. (2011) studied the optimal design and integration of ASU with IGCC systems, and the results showed that it can help to improve the efficiency and net power generation of an IGCC system with CCS. Wang et al. (2016) proposed a simultaneous optimization and integration method for the system of ASU and GT to improve efficiency of IGCC systems, and two improved case showed that additional 10% and 14% net power generation compared with traditional case, respectively. Han et al. (2017) developed a thermodynamic model for a 400 MW plant coupled with an elevated pressure air separation unit and examined the performance under various integrations to get the optimum solution. The results showed that the optimum solution was integrated with an air extraction rate of 80% and full nitrogen injection.

The second approach is to design and improve the efficiency of ASU, which provides oxygen and nitrogen to gasifier and combustor respectively. Cryogenic ASU is an important unit which significantly effects the overall efficiency and cost of IGCC systems (Fu et al., 2016a). Hence, improving the efficiency of cryogenic ASU is very necessary. Ham and Kjelstrup (2010) used exergy analysis to evaluate two process (with two or three distillation columns) designs of ASU, and the results showed that the three columns design destroyed 12% less exergy than the two columns design. Fu et al. (2016a) proposed an elevated-pressure cryogenic ASU for IGCC based on self-heat recuperation technology, and the energy requirement of the proposed ASU was reduced by 11% compared with traditional ASU.

The third approach is to optimize and integrate the IGCC system as a whole which is most effective because it directly improves overall energy efficiency without any other impact. Christou et al. (2008) studied the parametric cost–benefit analysis of IGCC technology (with or without CCS) and calculated the electricity unit cost of different power generation approaches. Lee et al. (2009) analyzed the impact of the design options on the performance of an IGCC system, including the technology of integrating a GT with an ASU and the degree of nitrogen supply from the ASU to the combustor. Al-Zareer et al. (2016, 2018) optimized an IGCC system from energy and exergy efficiencies and cost of the produced hydrogen and electricity based on genetic algorithm, and the optimization demonstrated that the IGCC system is cheaper to produce hydrogen and electricity.

The last approach is to integrate CCS with IGCC systems. IGCC is an innovative system that facilitates the implementation of CCS which can effectively reduce greenhouse gas emissions and reduce environmental pollution from fossil fuel combustion. In the gas clean-up subsystem, CO_2 can be separated from the syngas by adsorbent. Descamps et al. (2008) developed an evaluation method of CO_2 removal in an existing IGCC system which is based on an oxygen blown entrained flow gasifier and the efficiency of the IGCC system is 43%. Hoffmann and Szklo (2011) analyzed the maturity and costs of IGCC systems (with or without CCS) and assessed the influence of IGCC systems risk on economic viability, and the results showed that the introduction of IGCC systems with CCS on a wider scale faces large uncertainties.

Most papers focus on improve efficiency of complex system by more accurate control methods and algorithms. Liszka and Tuka (2012) studied whether the integration of air-side ASU-GT has a positive impact on the efficiency of IGCC, the results showed that the ASU-GT integration is not recommended from the efficiency point of view. Zhang et al. (2013) systematically analyzed the effect of Coal–water slurry (CWS) preheating gasification technology integration on the energy efficiency of wet IGCC system with and without carbon capture. The results showed that the total energy efficiency of the wet feed IGCC system without carbon capture is 1–5 percentage points (1%–5%) higher than that of the original wet feed IGCC system. Wang et al. (2015) established the mathematical model of IGCC device, including gasification device, air separation device and energy quality conversion combined cycle device. The Gibbs free energy minimization method is used to predict the composition of syngas and the efficient isentropic process is considered. Obara et al. (2016) established an IGCC numerical model to evaluate the electrical response characteristics, and studied the frequency characteristics of interconnected independent micro grid through numerical analysis. When the proposed IGCC system is installed with proportional integral differential controller and load tracking, even in the case of large-scale photovoltaic power waves, the energy flow through the micro grid is stable. Guan et al. (2019) introduced the particulate control devices (PCD) of IGCC project in Kemper County, which is the key component of Transport Integrated Gasification process. Kemper PCD is designed to accommodate different types of filter element optimization in the future. He and Lima (2019) proposed three model predictive control (MPC) strategies for coal-fired power plant cycling applications. The closed-loop results show that the control performance of nonlinear MPC (NLMPC) is 96% higher than that of dynamic matrix control (DMC) in terms of the integral squared error (ISE) results. Guo and Chen used Tapio (Guo and Yan, 2018) decoupling model, differential GMM method and peak prediction model to analyze the impact of environmental regulation on carbon emissions, and found that there is a significant inverted U-shaped curve relationship between environmental regulation and CO_2 emissions and CO_2 emission intensity.

The optimization and integration of IGCC system includes the integration between ASU and GT, and between GT and power generator, which is a very complicated process. At present, compared with other systems such as natural gas combined cycle (NGCC) system and conventional coal-fired power plants, the energy efficiency of IGCC system is relatively low, but there is a lot of room for improvement and less environmental pollution for IGCC systems.

Therefore, based on the previous work (Xu et al., 2019a,b), some auxiliary devices, such as sulfur recovery device, heat recovery steam generator (HRSG) device and waste water recovery (WWR) device are integrated to the traditional IGCC system to integrate organically with the IGCC system, which greatly improves the energy efficiency and exergy efficiency of the IGCC system.

2. Overall description of ASU and IGCC system

2.1. Cryogenic air separation unit (ASU)

Industrial gases are important energy sources or feedstocks of modern industry (Ivkovic et al., 2015). The industrial gases described mainly refers to the three gases, oxygen (molecular symbol O_2), nitrogen (molecular symbol N_2) and argon (molecular symbol Ar). They play an important role in the economy. The oxygen (O_2) in industrial gases is mainly applied to petrochemical, aerospace, thermal power and ferrous metallurgy industry. The ferrous metallurgy making process requires a large amount of oxygen, which is generally produced by cryogenic ASUs (Fu et al., 2016b). The use of medical O_2 is an increasing market (Ebrahimi and Ziabasharhagh, 2017). Oxy-combustion is a promising technology to mitigate carbon dioxide (molecular symbol CO_2) emissions, particularly from coal-based power plants (Fu and Gundersen, 2012). Nitrogen (N_2), as an element of great technical importance, can be produced at cryogenic temperatures (about 100 K/−173 °C) with 1 ppm (parts per million) of impurities. High purity nitrogen is used as protective gas and carrier

gas in the manufacture of integrated circuits, semiconductors and electric vacuum devices, the carrier gas of chemical vapor deposition, etc. High purity nitrogen in the process of epitaxy, lithography, cleaning and evaporation, as the replacement, drying, storage and transportation of gas, requires purity of more than 100 ppm. In aerospace technology, liquid hydrogen filling system must first use of high purity nitrogen replacement, and then the high purity helium replacement (Kim et al., 2011).

The global industrial gases market has been showing a steady growth in recent years according to the reports from gas world Association and China Industrial Gases Industry Association. To reduce energy consumption per unit industrial gases, the demand for the large-scale ASU will increase rapidly. There are various technologies that are used for the air separation process, such as cryogenic distillation, magnetic air separation technology (MAST), Membrane Adsorption, Pressure Swing Adsorption (PSA) and Vacuum Pressure Swing Adsorption (VPSA) (Hashim et al., 2011; Smith and Klosek, 2001a). At present, as the most effective method to produce large quantities of high purity industrial gases is Claude cycle cryogenic separation according to boiling points. Multiple ASUs constitute an air separation island. Fig. 1 presents an air separation island. Multiple large-scale ASUs and their visualized digital mockup (DMU) are respectively shown in Fig. 1(a) and (b).

The large-scale cryogenic air separation unit (ASU) produces industrial gases for modern industry. Under the dual pressure of energy and resources, most enterprises develop from ASU towards Integrating gasification island (IGI), a typical example of which is IGCC.

2.2. Overall forward integrated design of IGCC

The Integrated Gasification Island (IGI) mainly includes ASU, coal gasification plant and power generation plant. The whole IGI can realize the power and raw materials needed for internal supply and export the usable products outwards, such as Oxygen, Nitrogen, Carbon monoxide and Hydrogen. The process of IGI are as follows: the ASU provides Oxygen directly to the gasification unit, and can also provide other products, such as liquid Nitrogen, liquid Oxygen, clean gas and so on. The raw coal needs to pass through the pretreatment unit, then enters the gasification unit, under the catalyst function becomes the coarse gas (mainly hydrogen and carbon monoxide). The remaining impurities are waste gas and waste residue, and the waste gas can enter the expansion unit of the ASU to do work. Coarse gas needs to be purified by a purification device to remove internal fine dust, hydrogen sulfide, sulfur dioxide, carbon dioxide and other impurities. Pure hydrogen and carbon monoxide can be obtained through separation devices. Under the action of burning fuel coal, the boiler produces steam, which can drive the steam turbine to do work, and also can drive the generator set to do work to generate the electrical energy needed for the operation of the whole device.

The IGCC system has the advantages of high efficiency, low emission and low water consumption, which is one of the important development directions of clean coal technology in China. The IGCC is explored and put forward, which can reduce the irreversible loss in the energy conversion process and realize the cascade utilization of energy by integrating the hydrocarbon classification gasification process and chemical chain combustion process of coal. The IGCC system mainly consists of cryogenic ASU, gasification system, combustor, compressor, GT and power generator, as shown in Fig. 2.

The oxygen and nitrogen required by the IGCC system are produced in the cryogenic ASU. Most of the air required for the cryogenic ASU is provided by the GT compressor. Air extraction from GT compressor is of great significance for the IGCC system which can be concluded as follows:

(a) GT compressor surge problem can be avoided (Liszka and Tuka, 2012),
(b) the energy consumption of main air compressor (MAC) is reduced.

The ASU adopts double distillation columns, including a high-pressure lower column (HPLC) and a low-pressure upper column (LPUC). Oxygen stream is produced in the bottom of the LPUC and compressed to about 6737 kPa in the oxygen compressor (OC), which is mainly used in the gasifier. Nitrogen stream from the top of LPUC is divided into two streams, one stream is called vent nitrogen used as instrument gas and clean gas. Another stream is compressed to about 3190 kPa and injected into the GT combustor.

The gasification system mainly consists of gasifier, gas clean-up system (GCS), sulfur recovery device, water–gas shift unit and CO_2 capture and storage (CCS). Coal and water react with high-pressure oxygen as gasification agent to produce raw gas in the gasifier, and the equations of reversible chemical reaction can be described as

$$C + 0.5O_2 \longleftrightarrow CO \quad (1)$$

$$CO + 0.5O_2 \longleftrightarrow CO_2 \quad (2)$$

$$H_2 + 0.5O_2 \longleftrightarrow H_2O \quad (3)$$

$$C + CO_2 \longleftrightarrow 2CO \quad (4)$$

$$C + H_2O \longleftrightarrow CO + H_2 \quad (5)$$

$$C + 2H_2 \longleftrightarrow CH_4 \quad (6)$$

$$CO + H_2O \longleftrightarrow CO_2 + H_2 \quad (7)$$

The Eq. (1) proves that coal gasification reaction is neither pyrolysis reaction nor combustion reaction, but oxygen deficient reaction. The raw gas from the gasifier firstly pass a gas clean-up system (GCS) consisting of water scrubber, COS hydrolysis unit and heat exchangers network (HEN). The GCS can remove acid gas in the raw gas, such as H_2S and CO_2. Sulfur recovery can be achieved by adding a sulfur recovery unit in GCS, which can reduce the production of pollution gas SO_2. Then the syngas mainly including hydrogen (H_2), water (H_2O) and carbon monoxide (CO) will be fed into the water–gas shift unit (WGSU). The main reaction in WGSU is Eq. (8). The generated CO_2 is captured and stored in the CGS unit and the remaining H_2 is supplied to the GT combustor.

$$H_2O + CO \longleftrightarrow CO_2 + H_2 \quad (8)$$

Compressor, turbine and combustor are the main units in the GT system. Ambient air passes through the GT compressor and becomes compressed air. The compressed air is divided into two streams, one stream enters into ASU and the other stream enters into combustor. Feed streams including compressed air (oxidizing agent), H_2 (fuel) and the high-pressure nitrogen from ASU react in the GT combustor to produce fuel gas of high temperature and high pressure. The fuel gas enters the GT and drives GT to do work. A shaft is used to connect the compressor and turbine. The GT drives the electricity generator to generate electricity. Exhaust gas from GT still has high temperature and pressure, which can be recovered by HRSG to generate electricity.

The advantages of proposed green IGCC system are as follows:

(1) High energy efficiency. The IGCC systems integrate several devices to form a closed-loop system, which can better adapt to the operation of multiple working conditions, avoid waste of resources and repetitive start-up.

(2) Large-scale equipment. The traditional units cannot meet the demands of industry. The total amount of gas generated by the new IGCC system is dozens of times higher than that of the traditional one.

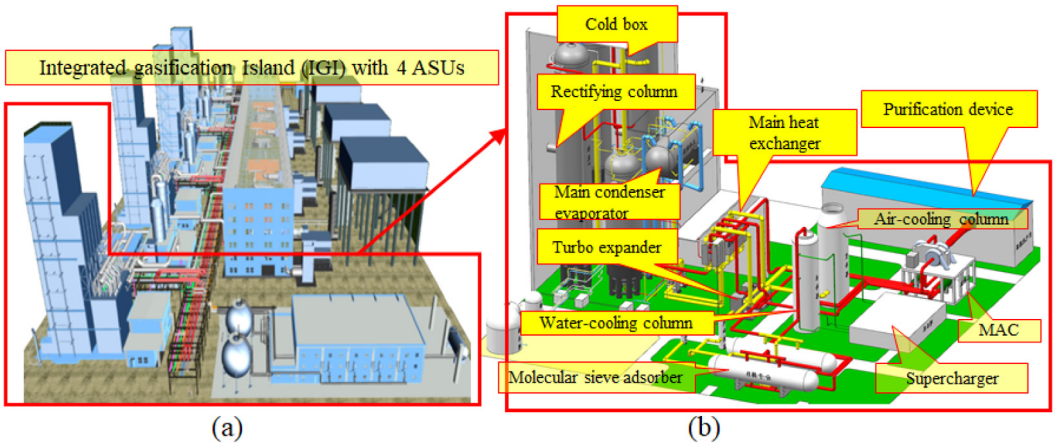

Fig. 1. Air separation island. (a) Multiple large-scale ASUs, (b) DMU of ASUs.

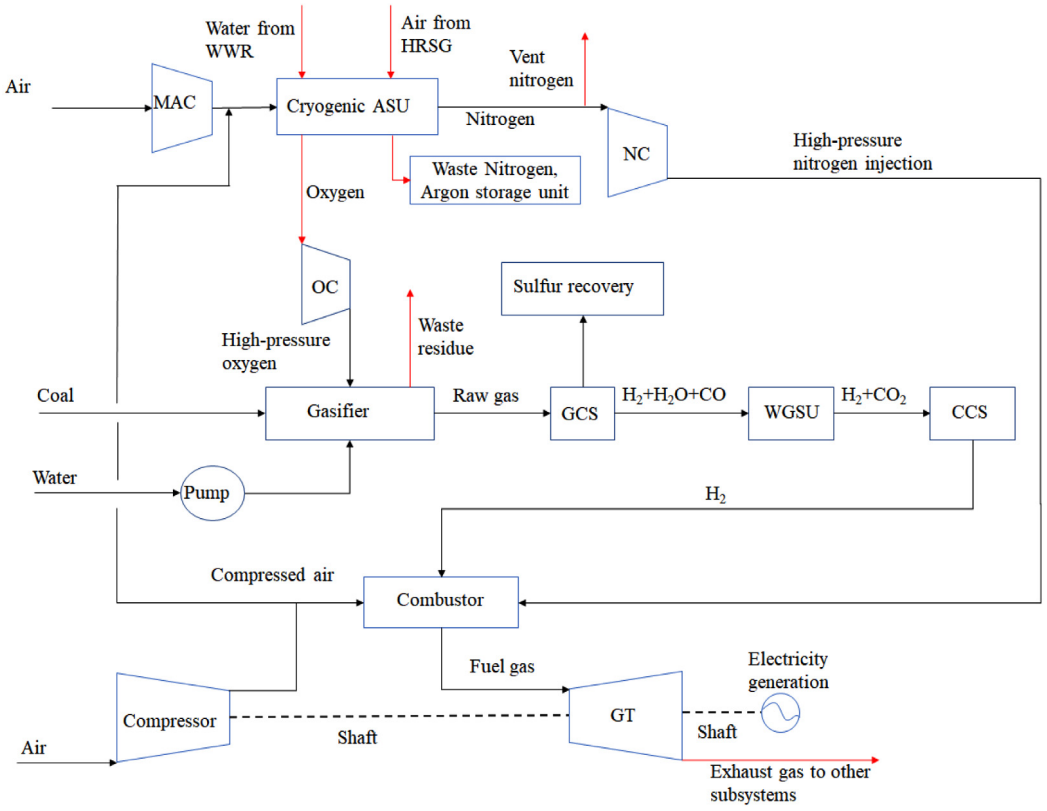

Fig. 2. Overall forward integrated design of IGCC.

(3) Low greenhouse gas (GHG) emission. The IGCC system converts coal into gas first, then burns in the combustor after purification. Compared with the traditional direct combustion method, its emission of pollutant gases such as NO_x and SO_x is very low, so it has less pollution to the environment. At the same time, sulfur recovery device is integrated to further desulfurization to reduce sulfur content in the syngas.

(4) Low water consumption. The IGCC system uses a WWR device to maximize the recovery of waste water discharged from the system, so that waste water reuse can effectively alleviate the shortage of water resources.

The fluid flow in the system is taken as the main variable and the whole system is designed and analyzed in combination with the working conditions. The heat recovery steam generator (HRSG), CO_2 capture and storage unit (CCS), waste water recovery (WWR) are integrated to the traditional system to improve the efficiency and the environmental performance of IGCC system. A green integrated gasification combined cycle (IGCC) system includes many devices, such as ASU, combustor, compressor, etc., as well as thousands of parameters, such as air flow $\dot{m}_{air}$, operating pressure P, compressor efficiency η, integration degree β, etc. It is necessary to give the definition of some parameters for the coupling between the units, which is convenient for design and analysis.

We define the integration degree β of ASU and IGCC and nitrogen supply ratio γ represent the extent of unit coupling, can be obtained as Eqs. (9) and (10).

$$\beta = \frac{\dot{m}_{air,GT}}{\dot{m}_{air,ASU}} \tag{9}$$

$$\gamma = \frac{\dot{m}_{N_2,GT}}{\dot{m}_{N_2,ASU}} \tag{10}$$

where β is integration degree; γ is nitrogen supply ratio; $\dot{m}_{air,GT}$ is the air mass flow rate to ASU from GT compressor (kg.s^{-1}); $\dot{m}_{air,ASU}$ is the total air mass flow rate to ASU (kg.s^{-1}); $\dot{m}_{N_2,GT}$ is the nitrogen mass rate supplied to GT combustor (kg.s^{-1}); $\dot{m}_{N_2,ASU}$ is the nitrogen mass rate separated from ASU (kg.s^{-1}).

3. Fundamentals of energy efficiency and exergy efficiency

3.1. Energy efficiency

In thermodynamics, the energy is a quantitative property, which can be stored, transmitted, conversed and utilized, equivalent to the capacity of a physical system to do work in a variety of forms, such as electrical, mechanical, chemical, thermal, or nuclear. The three laws of thermodynamics define physical quantities (temperature, energy, and entropy) that characterize thermodynamic systems at thermal equilibrium. The laws describe how these quantities behave under various circumstances, and preclude the possibility of certain phenomena (such as perpetual motion).

$$\Delta U = dQ - \delta W \quad \Delta U, dQ, \delta W \in R \tag{11}$$

where ΔU is internal energy change, dQ is amount of heat supplied to the closed system, δW is amount of work done by the system.

Most theories have been put forward to improve energy conversion efficiency. The Reversed Carnot cycle provides an upper limit on the efficiency that any system can achieve during the energy conversion. The Organic Rankine cycle (ORC) is an idealized thermodynamic cycle of a heat engine that converts heat into mechanical work while undergoing phase change.

For cryogenic ASU, the power consumption can be calculated as (Han et al., 2017).

$$E_{ASU} = E_{MAC} + E_{OC} + E_{NC} \tag{12}$$

where E_{ASU} is the power consumption of cryogenic ASU (MW); E_{MAC} is the power consumption of MAC (MW); E_{OC} is the power consumption of OC (MW); E_{NC} is the power consumption of nitrogen compressor NC (MW).

The net energy output of GT is given by

$$E_{net} = E_{GT} - E_{ASU} - E_{AU} \tag{13}$$

where E_{net} is the net power output (MW); E_{GT} is the GT power output (MW); E_{au} is the power consumption of auxiliary units (AU) (MW).

The IGCC net efficiency can be obtained as

$$\eta_{net} = \frac{E_{net}}{E_{coal}} \tag{14}$$

$$E_{coal} = \dot{m}_{coal} \times LHV \tag{15}$$

where η_{net} is the net efficiency of IGCC; E_{coal} is the coal consumption capacity of IGCC (MW); $\dot{m}_{coal}$ is the mass flow rate of coal (kg.s^{-1}); LHV is the coal low heating value (MJ.kg^{-1}).

The waste steam can pass the WWR device which includes heat exchangers and clean-up unit to get liquid water. Then the recovered water can feed into cryogenic or gasifier to reduce the external water supply.

$$\eta_{water} = \frac{\dot{m}_{water,recovered}}{\dot{m}_{water,total}} \tag{16}$$

where η_{water} is the efficiency of water recovery; $\dot{m}_{water,recovered}$ is the mass flow rate of recovered water (kg/s); $\dot{m}_{water,total}$ is the total mass flow rate of water (kg/s).

3.2. Exergy efficiency

Exergy can be defined as the quality of energy as it combines the first and second laws of thermodynamic. It is a more profound measure for analyzing energy process. An exergy analysis is the first step for the exergoeconomic analysis of energy conversion and energy-intensive chemical systems. The total exergy transfer rate $\dot{E}$ contained in a material stream can be decomposed into thermo-mechanical (or physical) exergy transfer rate $\dot{E}^{TM}$ and chemical exergy transfer rate $\dot{E}^{CH}$.

$$\dot{E} = \dot{E}^{TM} + \dot{E}^{CH} = \dot{m}(e^{TM} + e^{CH}) \tag{17}$$

where $\dot{E}$ is the exergy transfer rate (kW); $\dot{E}^{TM}$ is the thermo-mechanical exergy transfer rate (kW); $\dot{E}^{CH}$ is the chemical exergy transfer rate (kW); $\dot{m}$ is the mass flow rate (kg.s^{-1}); e^{TM} is the specific thermo-mechanical exergy (kJ.kg^{-1}); e^{CH} is the specific chemical exergy (kJ.kg^{-1}).

The specific thermo-mechanical exergy e^{TM} of a material stream can be given as:

$$e^{TM} = [h(T,P) - h(T_0,P_0)] - T_0[s(T,P) - s_0(T_0,P_0)] \tag{18}$$

where h is the specific enthalpy (kJ.kg^{-1}); s is the specific entropy (kJ.kg^{-1}.K^{-1}); P is pressure (MPa); T_0, P_0 are respectively the temperature (K) and pressure (MPa) of external ambient.

The specific thermo-mechanical exergy e^{TM} can be further decomposed into two components. One is thermal exergy (e^T) based on temperature and the other one is mechanical exergy (e^P) based on pressure. The decomposition is not unique and does not have a fundamental meaning, it makes it easier to analyze the exergy transfer within processes.

$$e^{TM} = e^T + e^P \tag{19}$$

$$e^T = [h(T,P) - h(T_0,P)] - T_0[s(T,P) - s_0(T_0,P)] \tag{20}$$

$$e^P = [h(T_0,P) - h(T_0,P_0)] - T_0[s(T_0,P) - s(T_0,P_0)] \tag{21}$$

where e^T is the specific thermal exergy (kJ.kg^{-1}); e^P is the specific mechanical exergy (kJ.kg^{-1}).

The exergy loss rate $\dot{I}$ can be calculated by setting up the exergy balance between all input and output exergy.

$$\dot{I} = \sum_{in} \dot{E} - \sum_{out} \dot{E} \tag{22}$$

where $\dot{I}$ is the exergy loss rate (kW).

The exergy efficiency can be defined as input–output exergy efficiency. The input–output exergy efficiency η_{exergy} is the ratio of the total output exergy to the total input exergy. It can be used for all process units when the total input exergy is transformed in to other components.

$$\eta_{exergy} = \frac{\dot{E}_{out}}{\dot{E}_{in}} \tag{23}$$

For IGCC in Fig. 2, exergy efficiency can be defined as

$$\eta_{exergy} = \frac{\dot{E}_{power}}{\dot{E}_{coal} + \dot{E}_{water} + \dot{E}_{air}} \tag{24}$$

where η_{exergy} is the exergy efficiency; $\dot{E}_{power}$ is the exergy of generator power (kW); $\dot{E}_{coal}$ is the exergy of coal (kW); $\dot{E}_{water}$ is the exergy of water (kW); E_{air} is the exergy of air (kW).

4. Mathematical model of predictive control

4.1. System identification from bigdata

The IGCC system has features such as interlock protection, closed coupling, large time lag and non-linearity, however, faster

response speed and lower overshoot are always the unremitting pursuits. The IGCC system is a nonlinear large-scale complex system (LSCS) where temperature, pressure, flowrate and other technical parameters play an important role in the operation and performance. The Multiple Input Multiple Output (MIMO) system can generally be decomposed into multiple single input single output (SISO) sub-systems. For the certain logical process with intuitionistic flow chart, the Mason's Equation can be used to obtain transfer function. However, for most MIMO the relations between the input and output are complex and implicit. Due to the large number and complex structure of IGCC devices, it is difficult to establish a real-time control model of IGCC.

Let $\boldsymbol{X} = x_1, x_1, \ldots, x_N$ and $\boldsymbol{Y} = y_1, y_2, \ldots, y_M$ be the input (excitation) and output (response) of model, respectively. The decomposed model contains $N * M$ transfer functions. The transfer function $G_{i,j}(s)$ between input x_i and output y_j can be defined as

$$G_{i,j}(s) = \frac{Y(s)}{X(s)} = \frac{L(\boldsymbol{Y})}{L(\boldsymbol{X})} = \frac{b_0 + b_1 s + b_2 s^2 + \cdots + b_{n-1} s^{n-1}}{1 + a_0 s + a_1 s^2 + a_2 s^3 + \cdots + a_{n-1} s^n} \quad n \in R^+ \tag{25}$$

where L is Laplace transform from time-domain to frequency domain, s is complex variable, $a_0, a_0, \ldots, a_{n-1}$ *and* $b_0, b_0, \ldots, b_{n-1}$ are the coefficients. The highest order of the system is n. The value of n determines the integral order or fractional order.

Then, a vector $\boldsymbol{C}$ that represents the dynamic characteristics of the MIMO can be obtained by

$$\begin{aligned}\boldsymbol{C} = [&(b_0, b_0, \ldots, b_{n-1}, a_0, a_0, \ldots, a_{n-1})_{1*1}, \ldots,\\ &(b_0, b_0, \ldots, b_{n-1}, a_0, a_0, \ldots, a_{n-1})_{i*j}, \ldots,\\ &(b_0, b_0, \ldots, b_{n-1}, a_0, a_0, \ldots, a_{n-1})_{N*M}]^T\end{aligned} \tag{26}$$

For high-order transfer function, many model order reduction (MOR) methods can be employed to reduce complexity, such as optimal Hankel norm approximation, recursive least-squares method (RLS), clustering algorithm, etc.

In the field of sampling bigdata, the sampling period is ΔT, the sampling times are N_0, and all the input and output recorded are superposed respectively, as shown in Eq. (27). In this way, the identification problem is transformed into the problem of solving $2n * N * M$ coefficients represented by Eq. (26) according to input $\boldsymbol{X}$ and output $\boldsymbol{Y}$ column vectors. It can be solved by Recursive Least Square (RLS) identification method.

$$\begin{cases}\boldsymbol{X} = \left[x_{1,1}, \ldots, x_{1,N_0}, x_{2,1}, \ldots, x_{2,N_0}, \ldots, x_{N,1}, \ldots, x_{N,N_0}\right]^T\\ \boldsymbol{Y} = [y_{1,1}, \ldots, y_{1,N_0}, y_{2,1}, \ldots, y_{2,N_0}, \ldots, y_{M,1}, \ldots, y_{M,N_0}]^T\end{cases} \tag{27}$$

Using bigdata driven model identification technique, on the premise of determining the control model, let t_d be delay time, t_r be risetime, t_p be peak time, t_s be settling time, $\boldsymbol{\delta}_{overshoot}$ be overshoot. The overshoot (or maximum deviation) is one of the dynamic performance indexes of the control system. It is the response process curve of the linear control system under the step signal input, which is also an index value of the step response curve to analyze the dynamic performance. Deviation refers to the difference between the adjusted parameter and the given value. For a stable constant value regulating system, the biggest deviation of the transition process is the difference between the first peak value of the adjusted parameter and the given value. During y (∞) is equal to the stable value, $\boldsymbol{\delta}_{overshoot}$ can be calculated by Eq. (28).

$$\boldsymbol{\delta}_{overshoot} = \frac{\boldsymbol{y}_{tp} - \boldsymbol{y}_{\infty}}{\boldsymbol{y}_{\infty}} \times 100\% \tag{28}$$

where $\boldsymbol{\delta}_{overshoot}$ is the overshoot of model; $\boldsymbol{y}_{tp}$ is the peak value of signal output; $\boldsymbol{y}_{\infty}$ is the stable value of output.

The essence of intelligent control is to keep balance between rapid response time and lower overshoot. There are many PID (Proportion Integration Differentiation) parameter tuning methods, such as critical proportioning method (Ziegler–Nichols or Z–N method), Damping oscillatory method, robust PID Parameter Tuning method and Integral Squared Time-weighted Errors (ISTE) optimal Parameter Tuning method. For traditional PID tuning control strategy, classic PID calculation formula is shown as

$$u(t) = K_P\left[e(t) + \frac{1}{T_I}\int_0^t e(t)\,dt + T_D\frac{dg(t)}{dt}\right] + u_{con} \tag{29}$$

where $u(t)$ is the controllable parameter; $e(t)$ is the deviation; K_P is the proportionality coefficient; T_I is the integration time constant (s); T_D is the differential time constant (s); u_{con} is control constant.

However, the model has some shortcomings, such as excessive overshoot, frequent fluctuations and so on.

4.2. Fuzzy supervisory predictive control

Considering the overall composition of the IGCC device and the complex nonlinear characteristics of the device control system, a low overshoot Fuzzy supervisory predictive control (FSPC) method is proposed. The IGCC control model is obtained from the combination of "off-line" and "on-line". Based on the parameters of historical IGCC device, the control model is continuously optimized. In order to achieve better performance, the coupling and collaborative control between various devices of IGCC need higher robustness under perturbation. The control system of IGCC requires fast tracking, small overshoot and adaptive off design capability.

The model of plant can be described.

$$\mathrm{A}\left(z^{-1}\right)\mathbf{Y}(t) = \mathrm{B}\left(z^{-1}\right)\boldsymbol{X}(t) + C\left(z^{-1}\right)v_e(t) + \frac{N_e\left(z^{-1}\right)}{\Delta} \tag{30}$$

$$\mathrm{A}\left(z^{-1}\right) = 1 + a_1 z^{-1} + a_2 z^{-2} + \cdots + a_{na} z^{-na} \tag{31}$$

$$\mathrm{B}\left(z^{-1}\right) = 1 + b_1 z^{-1} + b_2 z^{-2} + \cdots + b_{nb} z^{-nb} \tag{32}$$

$$\mathrm{C}\left(z^{-1}\right) = 1 + c_1 z^{-1} + c_2 z^{-2} + \cdots + c_{nc} z^{-nc} \tag{33}$$

$$\Delta = 1 - z^{-1} \tag{34}$$

where N_e is the Gaussian distribution with zero mean; z^{-1} is backward shift operator about t; Δ is forward difference operator; $N_e\left(z^{-1}\right)/\Delta$ is unmeasurable disturbance while v_e is measurable disturbance.

The model of adjustment layer can be described

$$\mathrm{A}_c\left(z^{-1}\right)\boldsymbol{X}(t) = \mathrm{B}_{cr}\left(z^{-1}\right)r(t) + \mathrm{B}_{cy}\left(z^{-1}\right)\boldsymbol{Y}(t) \tag{35}$$

$$\mathrm{A}_c\left(z^{-1}\right) = 1 + a_{c1} z^{-1} + \cdots + a_{cna} z^{-cna} \tag{36}$$

$$\mathrm{B}_{cr}\left(z^{-1}\right) = b_{r0} + b_{r1} z^{-1} + b_{r2} z^{-2} + \cdots + b_{rnb} z^{-rnb} \tag{37}$$

$$\mathrm{B}_{cy}\left(z^{-1}\right) = b_{y0} + b_{y1} z^{-1} + b_{y2} z^{-2} + \cdots + b_{ynb} z^{-ynb} \tag{38}$$

where r means the optimal value of adjustment layer.

The model of supervisory optimization layer can be described

$$\begin{aligned}J = &\sum_{\Delta t=1}^{n} Q_{\Delta t}\left[\hat{\boldsymbol{Y}}(t + \Delta t|t) - W(t + \Delta t)\right]^2\\ &+ \gamma\left[\hat{\boldsymbol{Y}}(t+1|t) - \hat{\boldsymbol{Y}}(t)\right] + \sum_{i=1}^{m}\lambda_i \times [\Delta\boldsymbol{X}(t+i\\ &-1) - \Delta v(t+i-1)]^2 + \sum_{i=1}^{m}\xi_i\boldsymbol{X}(t+i-1)\end{aligned} \tag{39}$$

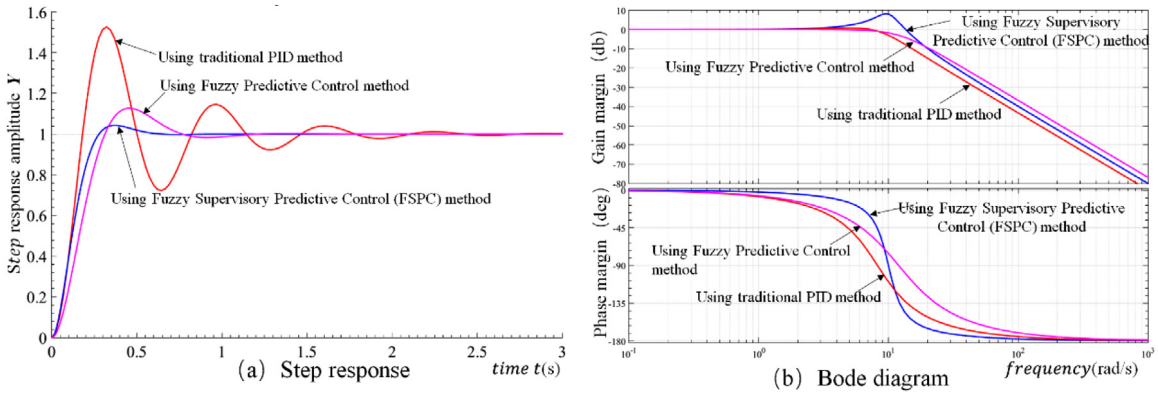

Fig. 3. Fuzzy Supervisory Predictive Control (FSPC) of unit in IGCC.

where J is the objective function; W is external reference assignment; $\hat{\boldsymbol{Y}}(t+\Delta t|t)$ is the predicted $\hat{\boldsymbol{Y}}(t+\Delta t)$ based on t; $\boldsymbol{X}(t+i-1)$ is the adjustable variable, $i = 1,2,\ldots,m$; $\Delta\boldsymbol{X}(t+i-1)$ is the increment of the adjustable variable, $i = 1,2,\ldots,m$; $\Delta v(t+i-1)$ is the increment of the measurable disturbance, $i = 1,2,\ldots,m$; n is the prediction domain; m is the control domain. $m = n$; Q, λ, ξ is the positive definite matrix of weight coefficient.

The fuzzy rules extracted from historical bigdata are employed in supervisory layer to make the precise control decisions. The control model consists of c rule bases. Each rule is divided into rule antecedent and rule antecedent. The ith rule is as follows:

$$\begin{aligned}&\boldsymbol{R}^i: if\ \ x_{1,t}\ \ is\ \ A^i_{1,t}\cdots and\ x_{m,t}\ \ is\ \ A^i_{m,t}\\ &\quad then\ \ y^i_t = p^i_0 + p^i_1 x_{1,t} + \cdots + p^i_m x_{m,t}\end{aligned} \tag{40}$$

where $i = 1,2,\ldots,c$ is the number of fuzzy rule bases; $x_{i,t}$ is the input of the tth model; y^i_t is the output of tth model under ith rule; A^i_j is fuzzy theory domain and main parameters of rule antecedent, which can be obtained by clustering method; $p_0, p_1 \cdots p_m$ are the parameters of rule consequent which can be obtained by least square (LS) method.

In supervisory layer, the fuzzy output y_t of the fuzzy model at the tth moment is as follows:

$$y_t = \frac{\sum_{i=1}^{c} f^i y^i_t}{\sum_{i=1}^{c} f^i} \tag{41}$$

where y_t is the fuzzy output of model at the tth moment; f^i is the membership function of ith rule.

The Fuzzy Supervisory Predictive Control (FSPC) of unit in IGCC is shown in Fig. 3. From Fig. 3(a), using traditional PID method, t_d is 0.1151 s, t_r is 0.1842 s, t_p is 0.3224 s, t_s is 1.9572 s, $\delta_{overshoot}$ is 52.1857%. Using Fuzzy Predictive Control method, t_d is 0.1630 s, t_r is 0.3158 s, t_p is 0.4585 s, t_s is 0.7030 s, $\delta_{overshoot}$ is 12.5054%. Using FSPC method, t_d is 0.1248 s, t_r is 0.2823 s, t_p is 0.3691 s, t_s is 0.4940 s, $\delta_{overshoot}$ is 4.5197%. From Fig. 3(b), Bode diagram about frequency response of dynamic systems, using traditional PID method, the gain margin is ∞, the phase margin is 32.8443. Using Fuzzy Predictive Control method, the gain margin is ∞, the phase margin is 101.7767. Using FSPC method, the gain margin is ∞, the phase margin is 178.0085. The infinite gain margin indicates the stability of the system. The larger the phase margin is, the more stable the system is.

5. Improving energy and exergy efficiency of IGCC system

The IGCC system integrates many advanced technologies, such as coal gasification, gas clean-up technology, GT technology and steam turbine (ST) technology. It is a promising technology to improve energy efficiency. The integration of IGCC systems with other devices or systems has been widely studied. Smith and Klosek (2001b) introduced air separation technologies and their integration with energy conversion process in detail. Cormos (2010) introduced the energy consumption of IGCC systems with CCS which is expected to play an important role in the future for decreasing greenhouse gas emissions. Asif et al. (2015) used exergy analysis to analyze three kinds of IGCC systems (IGCC without CCS, IGCC with pre-combustion CCS and IGCC with post-combustion CCS, and the results showed that IGCC with post-combustion CCS is more efficient. Duan et al. (2015) proposed an IGCC system with less CO_2 emission by integrating a Molten Carbonate Fuel Cell (MCFC) for CO_2 capture. Al-Zareer et al. (2016) proposed a new IGCC with a water–gas shift membrane reactor. The propose of integration is mainly to improve the efficiency of IGCC. In the design of IGCC system, the integration of ASU and IGCC and the integration of HRSG and IGCC system are adopted and also includes WWR, sulfur recovery and CCS. The commercial software Aspen Plus is used to simulate the IGCC system using Peng–Robinson equation as the state.

5.1. Energy efficiency ASU in IGCC system

For IGCC, the main unit of energy consumption is ASU which is up to 15% energy consumption. Meanwhile, For ASU, the main unit of energy consumption is MAC. Therefore, the working state control of MAC plays an important role in reducing energy consumption of IGCC.

According to thermodynamics, the critical pressure and temperature of water are respectively 22.12 MPa and 374.15 °C. By definition, subcritical state means below a critical threshold. When the pressure and temperature of steam are greater than the critical parameters, it can be called supercritical (SC). The SC means the operating pressure of main steam pressure in the unit is greater than the critical pressure of water (22.12 MPa). Generally, the ultra-super critical (USC) means the operating pressure of main steam pressure is about 27–35 MPa or above, and the temperature of main steam is 580 °C or above.

Fig. 4 presents the ASU and GT integration system. The cryogenic ASU provides oxygen and nitrogen to GT and GT compressor provides compressed air to ASU. The cryogenic ASU adopts "one drags two" unit to reduce energy consumption. "One drags two" means one power-output shaft of turbine engine (ST or GT) connect MAC and turbo-expander. The main product parameters in ASU are listed in Table 1.

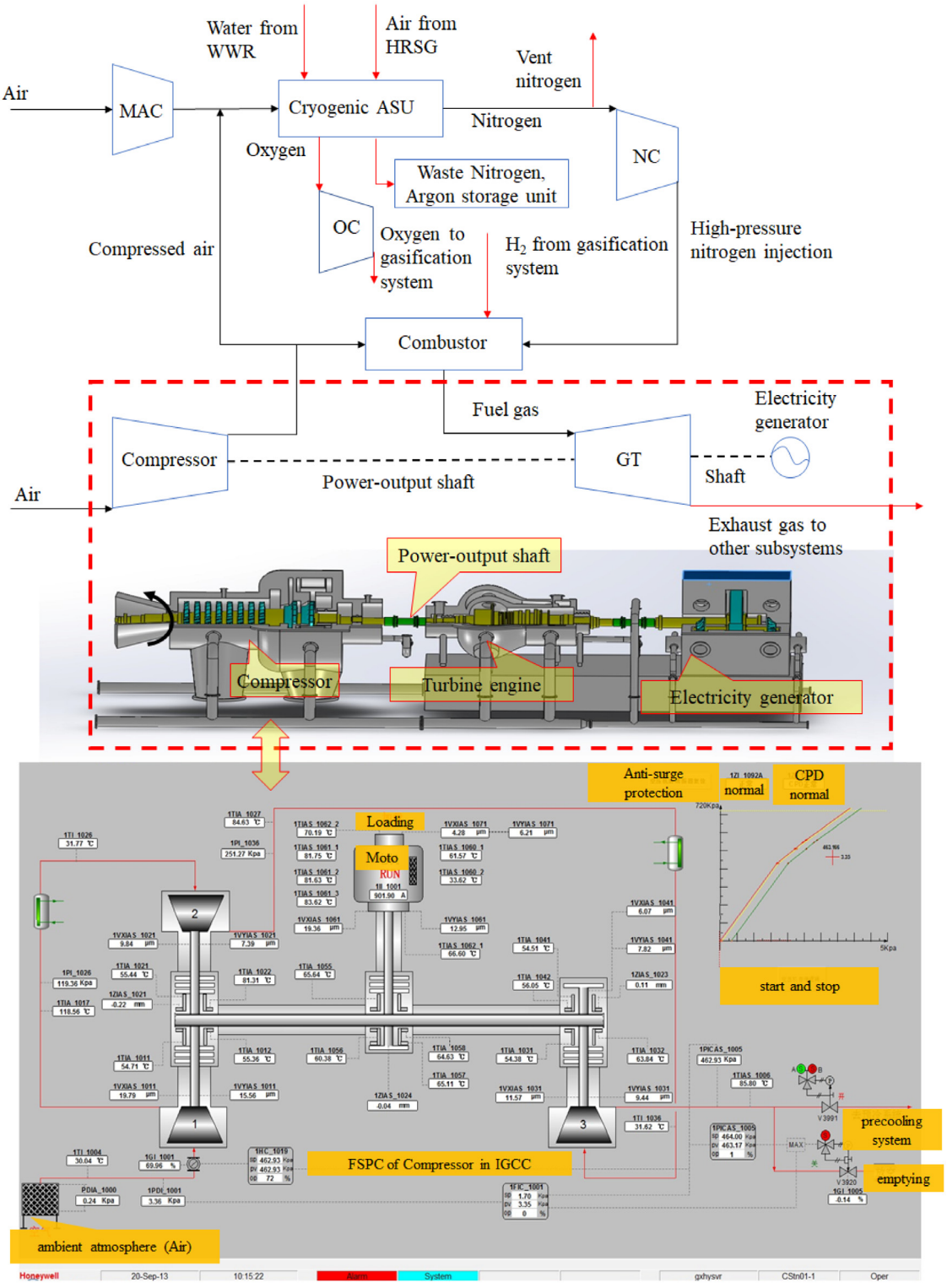

Fig. 4. ASU and GT in IGCC.

5.2. Fuzzy supervisory predictive control of HRSG and IGCC system

Fig. 5 presents the HRSG system of IGCC. In the IGCC system, each reaction process is carried out at higher or lower ambient temperature and ambient pressure, but the temperature and pressure of the final products will approach the ambient temperature and pressure, so it is an important method of energy conservation to recover the heat or cold energy stored in the products or waste streams. The exhaust gas from GT is still at high temperature and high pressure which can be further used in HRSG system. It consists of three kinds of ST including high-pressure steam turbine (HPST), intermediate-pressure steam turbine (IPST) and low-pressure steam turbine (LPST). Steam with different pressures can be effectively utilized. The main parameters of HRSG are listed in Table 2.

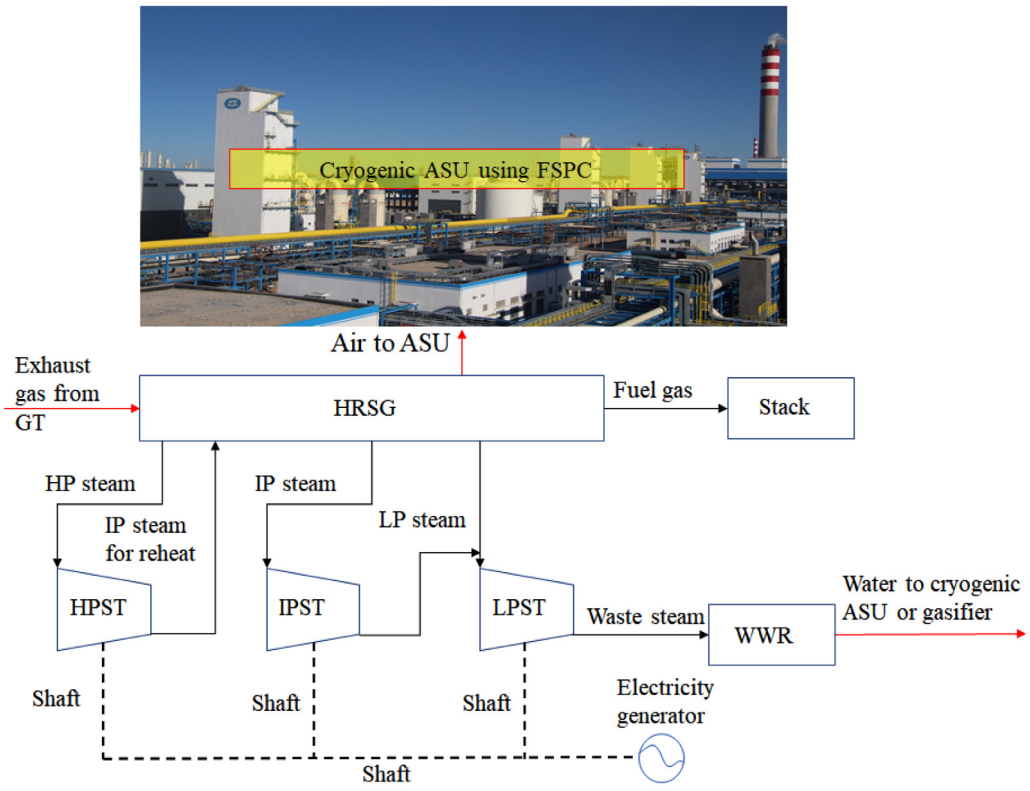

Fig. 5. HRSG and WWR in IGCC.

Table 1
Main product parameters in ASU.

IGCC parameters	Values using FSPC
Ambient air temperature T_0 (K)	288.2
Ambient air pressure P_0 (kPa)	101.3
Purity of oxygen	95 mol%
Purity of nitrogen	50 ppm O_2
Inlet pressure of OC $P_{OC,in}$ (kPa)	637
Outlet pressure of OC $P_{OC,out}$ (kPa)	6737
Inlet pressure of NC $P_{NC,in}$ (kPa)	1827
Outlet pressure of NC $P_{NC,out}$ (kPa)	3190
Compressor efficiency η_C	0.85

Table 2
Main parameters of HRSG and WWR.

IGCC parameters	Values using FSPC
Exhaust gas temperature from GT T_{EG} (K)	700
Inlet pressure of HPST $P_{HPST,in}$ (kPa)	14 000
Inlet temperature of HPST $T_{HPST,in}$ (K)	750
Inlet pressure of IPST $P_{IPST,in}$ (kPa)	4000
Inlet temperature of IPST $T_{IPST,in}$ (K)	599
Inlet pressure of LPST $P_{LPST,in}$ (kPa)	800
Inlet temperature of LPST $T_{LPST,in}$ (K)	488
Inlet pressure of WWR $P_{WWR,in}$ (kPa)	20
Isentropic efficiency of ST η_{ST}	0.90

Table 3
Properties of coal used in IGCC systems.

Proximate analysis	Mole fraction
Moisture	5.00%
Volatiles	5.00%
Fixed carbon	79.5%
Waste residue	10.50%
Ultimate analysis	**Mole fraction**
Carbon	78.97%
Hydrogen	2.63%
Oxygen	1.48%
Nitrogen	1.01%
Sulfur	0.36%
Chlorine	0.05%
LHV	29.92 MJ/kg

Table 4
The components of raw gas from coal combustion.

Components	Mole fraction
H_2	28.13%
CH_4	5.62%
CO	40.94%
CO_2	14.48%
H_2O	9.77%
N_2	1.06%

5.3. Reducing emissions of IGCC system by CCS using FSPC

The emissions of typical IGCC are mainly carbon dioxide, sulfides (mainly sulfur dioxide), nitrogen oxide (NOx) and waste water. The removal efficiency of emissions means the CO_2 capture rate, desulfurization efficiency and denitrification efficiency (denitration for coal gas). Fig. 6 presents the gasification system of IGCC. It consists of gasifier, GCS (desulfurization and denitrification system), sulfur recovery and CCS. The properties of coal used are listed in Table 3 (Han et al., 2017). High-pressure oxygen, coal and water react in the gasifier to produce raw gas. The components of raw gas are listed in Table 4 (Lee et al., 2009). Integration of CCS and IGCC can effectively reduce the greenhouse gas (GHG) emissions. Sulfur recovery is able to decrease the mole fraction of pollution gas H_2S and achieve sulfur recovery.

Fig. 7shows the effects of the initial concentration of (a) SO_2 and (b) NOx on deSO_2 and deNOx removal efficiencies. From Fig. 7(a), for desulfurization efficiency, the max is 91%, the min is 53%, the mean is 82.3%. For denitration efficiency the max is 98%,

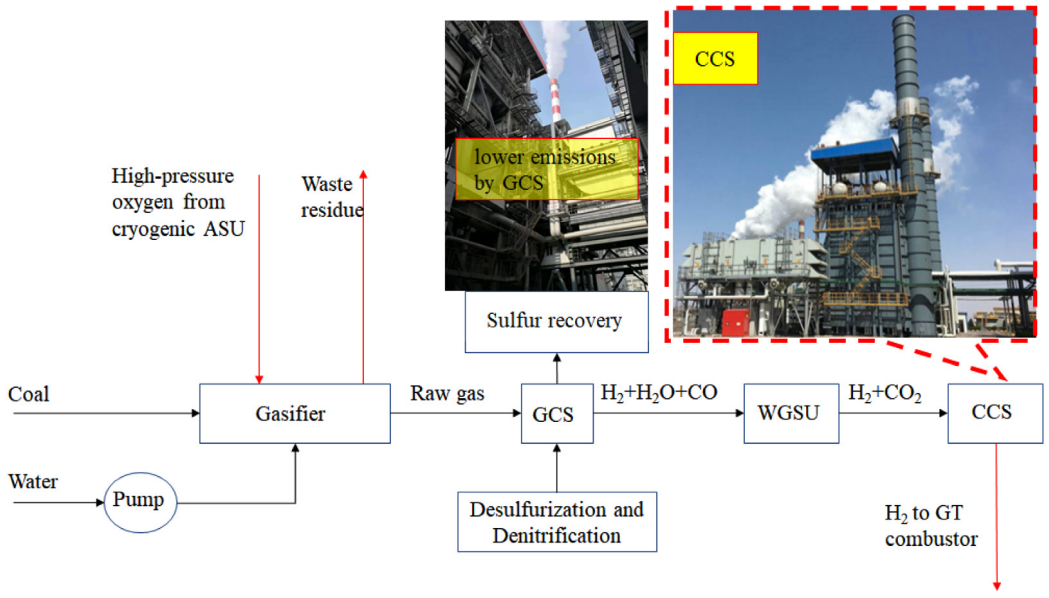

Fig. 6. CCS for reducing emissions in IGCC.

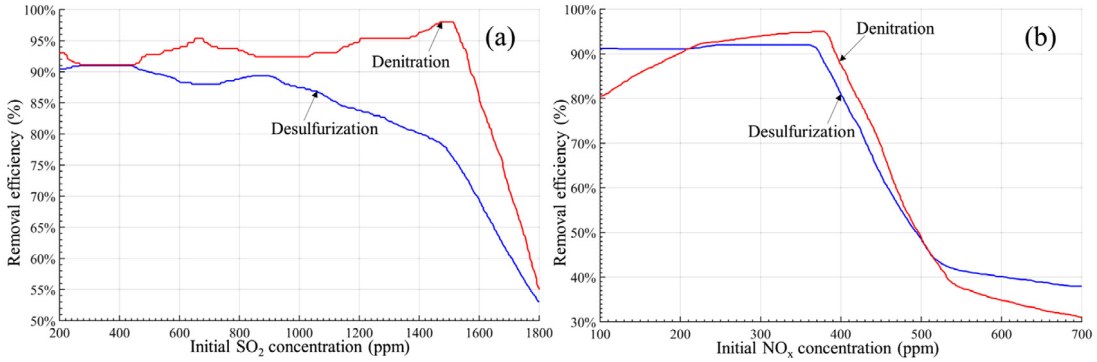

Fig. 7. Effects of the initial concentration of (a) SO_2 and (b) NOx on deSO_2 and deNOx removal efficiencies.

the min is 55%, the mean is 89.87%. From Fig. 7(b), for desulfurization efficiency, the max is 92%, the min is 38%, the mean is 69.2%. For denitration efficiency the max is 95%, the min is 30%, the mean is 69.71%. The desulfurization efficiency and denitrification efficiency are both above 90% and 60% respectively. Using FSPC on mass flow rate, initial concentration (ppm) and temperature, the total pressure loss of the GCS system is optimized from 3286 Pa to 2971 Pa which improves energy efficiency of IGCC system.

Fig. 8 shows the improved IGCC using FSPC with lower emissions. It shows that the maximum sulfur dioxide is less than 16.47 mg/N m^3 and the maximum nitrogen oxide NOx is less than 53.26 mg/N m^3.

6. Results and comparison

Taking the large-scale (300 MW) IGCC for example, considering the integration between different units and systems, the simulation analysis is carried out. The exergy loss rate of unit in IGCC before and after optimization is shown in Table 5.

The performances of IGCC system before and after using FSPC are shown in Table 6. The CO conversion rate and CO_2 absorption rate are decreased to 0 because of CCS. The GT efficiency η_{GT} is increased from 42.1% to 50.6% with the ratio of 20.2%. The efficiency of water recovery η_{water} is increased from 40.7% to 62.1% with the ratio of 52.6% because of WWR system. The net efficiency of IGCC system η_{net} is increased from 37.6% to 41.7% with the ratio of 10.9% because of the integration of different units and systems.

Table 5
Exergy loss rate of unit in IGCC before and after optimization.

Unit in IGCC	$\dot{I}$ (MW) before co-optimization	$\dot{I}$ (MW) after co-optimization	Ratio
Coal gasification	19	18.2	−4.2%
Purification	5.8	5.6	−3.4%
Compressor	5.1	4.9	−3.9%
Combustion chamber	21.2	20.3	−4.2%
Steam turbine (ST)	4.4	4.2	−4.5%
Gas turbine (GT)	2.9	2.8	−3.4%
ASU	8.8	8.4	−4.5%
CCS	2.2	2.1	−4.5%
WWR	1.5	1.4	−6.7%
HRSG	2.2	3.1	−4.5%
Total IGCC	73.1	70	−4.2%

Fig. 9 shows the efficiency performances of IGCC system before and after using FSPC.

The energy efficiency and exergy efficiency co-optimization of IGCC are shown in Fig. 10. Fig. 10(a) shows that the η_{net} firstly increases and then decreases with the increase of integration ratio β between ASU and IGCC. The η_{net} decreases with the increase of removal efficiency of emissions. Fig. 10(b) shows that η_{exergy} varies with nonmonotonic fluctuations about β and removal efficiency

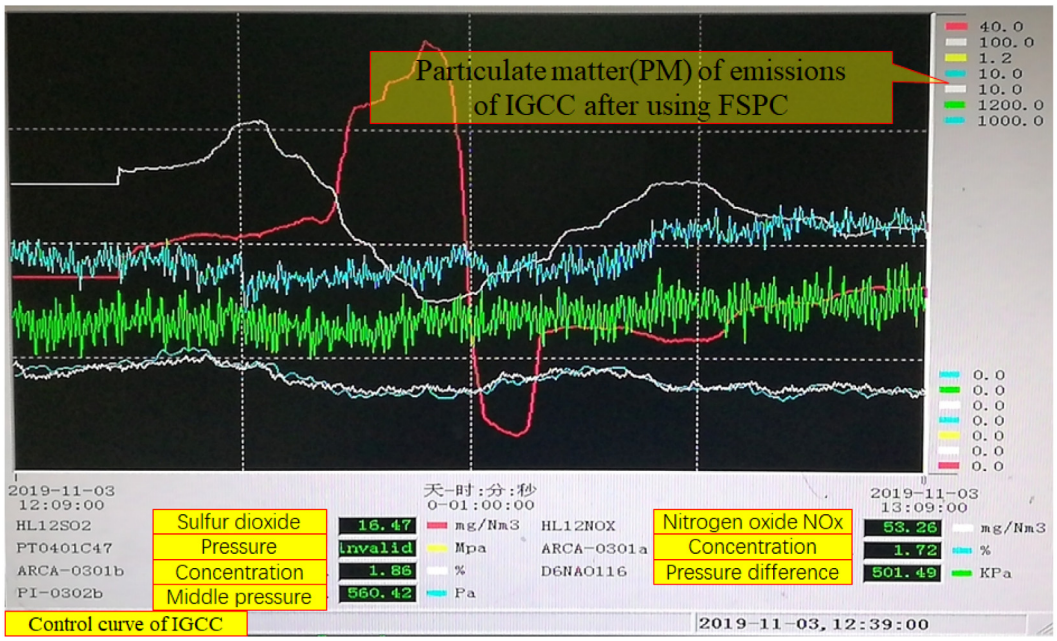

Fig. 8. The improved IGCC using FSPC with lower emissions.

Table 6
Performances of IGCC system before and after using FSPC.

IGCC parameters	Before using FSPC	After using FSPC	Ratio
Coal flow rate $\dot{m}_{coal}$ (kg.s^{-1})	30	30	0
CO conversion rate	90 mol%	0	−100%
CO_2 absorption rate	94 mol%	0	−100%
Integration ratio β	28.6%	35.5%	24.1%
Nitrogen supply ratio γ	71.2%	70%	−1.7%
GT efficiency η_{GT}	42.1%	50.6%	20.2%
GT power output E_{GT} (MW)	469.5	508.3	8.3%
Efficiency of water recovery η_{water}	40.7%	62.1%	52.6%
Net efficiency of IGCC system η_{net}	37.6%	41.7%	10.9%
Exergy efficiency of IGCC system η_{exergy}	36.5%	39.2%	7.4%

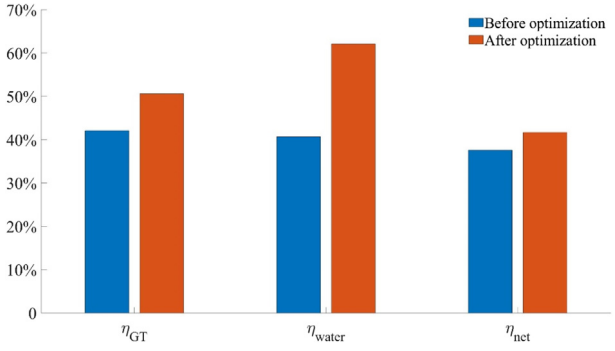

Fig. 9. Efficiency performance of IGCC system before and after optimization.

of emissions. The addition of purification devices might reduce the economy of the system but with lower emissions.

Fig. 11 shows the running IGCC based on fuzzy supervisory predictive control (FSPC).

7. Conclusions

(1) An energy and exergy co-optimization method of integrated gasification combined cycle (IGCC) based on Fuzzy Supervisory Predictive Control

The Fuzzy Supervisory Predictive Control (FSPC) method is proposed to implement robust control under complex disturbances by pre-considering unmeasurable disturbance and measurable disturbance. The fuzzy rules extracted from historical bigdata are employed in supervisory layer to make the precise control decisions. The proposed method has great significance for the energy-saving and Near-zero emissions (NZEC) IGCC with high safety and robust control by improving desulfurization efficiency and denitrification efficiency.

(2) An IGCC process is proposed which contains three principle couplings: ASU, heat recovery steam generator (HRSG) and CO_2 capture /storage unit (CCS)

FSPC is proposed to improve robustness of unit in IGCC under supercritical (SC) or ultra-super critical (USC) state. Integrating gasification island (IGI) is the trend of large-scale cryogenic ASU. The cryogenic ASU is coupled with gas turbine (GT) to save energy by improving the net energy output of GT. The Integration of CCS and IGCC can effectively reduce the greenhouse gas (GHG) emissions.

(3) The net efficiency of IGCC system is increased from 37.6% to 41.7% with the ratio of 10.9%. The exergy efficiency of IGCC system is increased from 36.5% to 39.2% with the ratio of 7.4%

Taking the large-scale (300 MW) IGCC for example, after using IGCC, the efficiency of water recovery is increased from 40.7% to 62.1% with the ratio of 52.6% because of waste water recovery (WWR) system. The feedstocks conservation with low carbon emissions can be realized by using FSPC. This is meaningful especially in relatively water-shortage dry areas and for industry with massive waste heat. It is of great significance for high safety and high efficiency IGCC and other complex industrial process system under supercritical (SC) or ultra-super critical (USC) state.

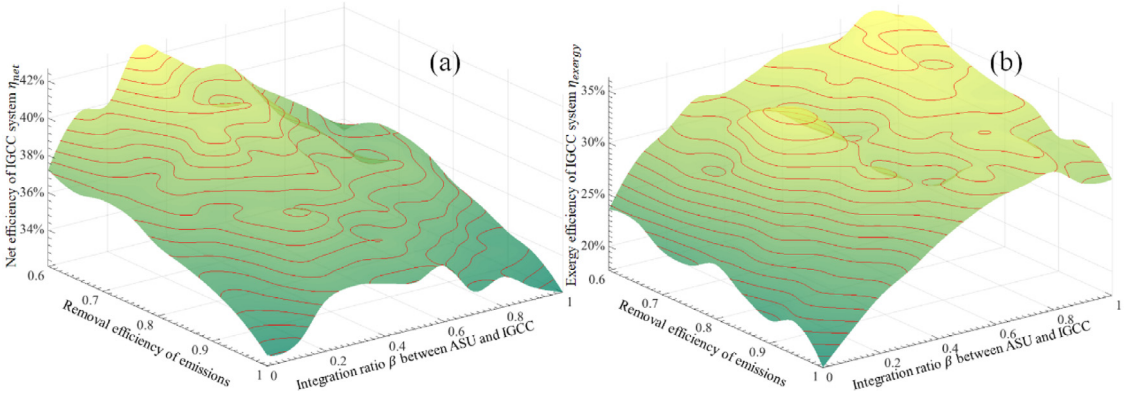

Fig. 10. Energy efficiency and exergy efficiency co-optimization of IGCC.

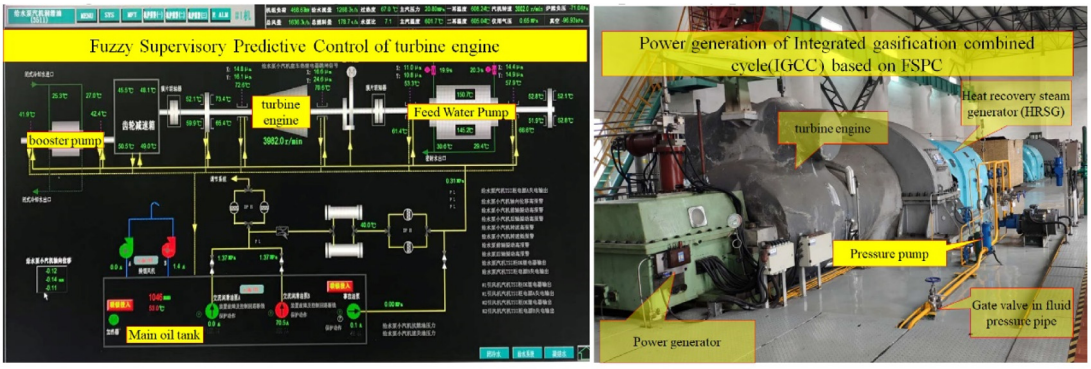

Fig. 11. The running IGCC based on fuzzy supervisory predictive control (FSPC).

Nomenclature

$e\,(t)$ is the deviation;
e^{CH} is the specific chemical exergy (kJ.kg^{-1});
e^{TM} is the specific thermo-mechanical exergy (kJ.kg^{-1});
e^{P} is the specific mechanical exergy (kJ.kg^{-1});
e^{T} is the specific thermal exergy (kJ.kg^{-1});
$\dot{E}$ is the exergy transfer rate (kW);
$\dot{E}_{air}$ is the exergy of air (kW);
$\dot{E}_{coal}$ is the exergy of coal (kW);
$\dot{E}^{CH}$ is the chemical exergy transfer rate (kW);
$\dot{E}_{power}$ is the exergy of generator power (kW);
$\dot{E}_{water}$ is the exergy of water (kW);
E_{AU} is the power consumption of auxiliary units (MW);
E_{ASU} is the power consumption of cryogenic ASU (MW);
E_{coal} is the coal consumption capacity of IGCC (MW);
E_{GT} is the power output of GT (MW);
E_{MAC} is the power consumption of MAC (MW);
E_{net} is the net power output (MW);
E_{NC} is the power consumption of NC (MW);
E_{OC} is the power consumption of OC (MW);
J is the objective function;
h is the specific enthalpy (kJ.kg^{-1});
$\dot{I}$ is the exergy loss rate (kW);
K_P is the proportionality coefficient;
L is Laplace transform from time-domain to frequency domain;
LHV is the coal low heating value (MJ.kg^{-1});
$\dot{m}$ is the mass flow rate (kg.s^{-1});
$\dot{m}_{air,ASU}$ is the total air mass flow rate to ASU (kg.s^{-1});
$\dot{m}_{air,GT}$ is the air mass flow rate to ASU from GT compressor (kg.s^{-1});
$\dot{m}_{coal}$ is the mass flow rate of coal (kg.s^{-1});
m_i is differential order of PDE;
$\dot{m}_{N_2,ASU}$ is the nitrogen mass rate separated from ASU (kg.s^{-1});
$\dot{m}_{N_2,GT}$ is the nitrogen mass rate supplied to GT combustor (kg.s^{-1});
$\dot{m}_{water,recovery}$ is the mass flow rate of recovered water (kg.s^{-1});
$\dot{m}_{water,total}$ is the total mass flow rate of water (kg.s^{-1});
N_e is the Gaussian distribution with zero mean;
P is pressure (MPa);
P_0 is the ambient air pressure (kPa);
$P_{HPST,in}$ is the inlet pressure of HPST (kPa);
$P_{IPST,in}$ is the inlet pressure of IPST (kPa);
$P_{LPST,in}$ is the inlet pressure of LPST (kPa);
$P_{NC,in}$ is the inlet pressure of NC (kPa);
$P_{NC,out}$ is the outlet pressure of NC (kPa);
$P_{OC,in}$ is the inlet pressure of OC (kPa);
$P_{OC,out}$ is the outlet pressure of OC (kPa);
$P_{WWR,in}$ is the inlet pressure of WWR (kPa);
s is the specific entropy (kJ.kg^{-1}.K^{-1});
t is time (s);
T_0 is the ambient air temperature (K);
T_D is the differential time constant (s);
T_{EG} is the temperature of exhaust gas from GT (K);
$T_{HPST,in}$ is the inlet temperature of HPST (K);
T_I is the integration time constant (s);
$T_{IPST,in}$ is the inlet temperature of IPST (K);
$T_{LPST,in}$ is the inlet temperature of LPST (K);
u_{con} is control constant;
$u\,(t)$ is the controllable parameter;
v_e is measurable disturbance;
W is external reference assignment;

$\boldsymbol{y}_{tp}$ is the maximum value of signal output;
$\boldsymbol{y}_{\infty}$ is the stable value of output;
z^{-1} is backward shift operator about t;
β is integration degree;
γ is nitrogen supply ratio;
$\boldsymbol{\delta}_{overshoot}$ is the overshoot of response;
Δ is forward difference operator;
η_C is the compressor efficiency;
η_{exergy} is the exergy efficiency;
η_{net} is the net efficiency of IGCC;
η_{water} is the efficiency of water recovery;

Declaration of competing interest

The authors declare that they have no known competing financial interests or personal relationships that could have appeared to influence the work reported in this paper.

Acknowledgments

The work presented in this article is funded by the National Natural Science Foundation of China (Nos. 51775494; 51935009; 51821093), National key research and development project of China (No. 2018YFB1700701), Zhejiang key research and development project of China (No. 2019C01141).

References

Al-Zareer, M., Dincer, I., Rosen, M.A., 2016. Modeling and performance assessment of a new integrated gasification combined cycle with a water gas shift membrane reactor for hydrogen production. Comput. Chem. Eng. 103, 275–292.
Al-Zareer, M., Dincer, I., Rosen, M.A., 2018. Multi-objective optimization of an integrated gasification combined cycle for hydrogen and electricity production. Comput. Chem. Eng. 117, 256–267.
Asif, M., Bak, C.U., Saleem, M.W., Kim, W.S., 2015. Performance evaluation of integrated gasification combined cycle (IGCC) utilizing a blended solution of ammonia and 2-amino-2-methyl-1-propanol (AMP) for CO 2 capture. Fuel 160, 513–524.
Chen, Y.S., Hsiau, S.S., Shu, D.Y., 2018. System efficiency improvement of IGCC with syngas clean-up. Energy 152, 75–83.
Christou, C., Hadjipaschalis, I., Poullikkas, A., 2008. Assessment of integrated gasification combined cycle technology competitiveness. Renew. Sustain. Energy Rev. 12 (9), 2459–2471.
Cormos, C.C., 2010. Evaluation of energy integration aspects for IGCC-based hydrogen and electricity co-production with carbon capture and storage. Int. J. Hydrogen Energy 35 (14), 7485–7497.
Descamps, C., Bouallou, C., Kanniche, M., 2008. Efficiency of an integrated gasification combined cycle (IGCC) power plant including CO removal. Energy 33 (6), 874–881.
Duan, L., Sun, S., Yue, L., Qu, W., Yang, Y., 2015. Study on a new IGCC (integrated gasification combined cycle) system with CO 2 capture by integrating MCFC (molten Carbonate fuel cell). Energy 87 (1), 490–503.
Ebrahimi, A., Ziabasharhagh, M., 2017. Optimal design and integration of a cryogenic air separation unit (ASU) with liquefied natural gas (LNG) as heat sink, thermodynamic and economic analyses. Energy 126, 868–885.
Emun, F., Gadalla, M., Majozi, T., Boer, D., 2010. Integrated gasification combined cycle (IGCC) process simulation and optimization. Comput. Chem. Eng. 34 (3), 331–338.
Fu, C., Gundersen, T., 2012. Using exergy analysis to reduce power consumption in air separation units for oxy-combustion processes. Energy 44 (1), 60–68.
Fu, Q., Kansha, Y., Song, C., Liu, Y., Ishizuka, M., Tsutsumi, A., 2016a. An elevated-pressure cryogenic air separation unit based on self-heat recuperation technology for integrated gasification combined cycle systems. Energy 103, 440–446.
Fu, Q., Kansha, Y., Song, C., Liu, Y., Ishizuka, M., Tsutsumi, A., 2016b. A cryogenic air separation process based on self-heat recuperation for oxy-combustion plants. Appl. Energy 162, 1114–1121.
Guan, X., Hewitt, A., Peng, W., Vimalchand, P., Nelson, M., Pinkston, T., Madden, D., 2019. Particulate control devices in Kemper County IGCC Project. Energy Rep. 5, 969–978.
Guo, W., Yan, C., 2018. Assessing the efficiency of China s environmental regulation on carbon emissions based on tapio decoupling models and GMM models. Energy Rep..
Ham, L.V.V.D., Kjelstrup, S., 2010. Exergy analysis of two cryogenic air separation processes. Energy 35 (12), 4731–4739.
Han, L., Deng, G., Li, Z., Wang, Q., Ileleji, K.E., 2017. Integration optimisation of elevated pressure air separation unit with gas turbine in an IGCC power plant. Appl. Therm. Eng. 110, 1525–1532.
Hashim, S.S., Mohamed, A.R., Bhatia, S., 2011. Oxygen separation from air using ceramic-based membrane technology for sustainable fuel production and power generation. Renew. Sustain. Energy Rev. 15 (2), 1284–1293.
He, X., Lima, F.V., 2019. Development and implementation of advanced control strategies for power plant cycling with Carbon Capture. Comput. Chem. Eng..
Hoffmann, B.S., Szklo, A., 2011. Integrated gasification combined cycle and carbon capture: A risky option to mitigate CO emissions of coal-fired power plants. Appl. Energy 88 (11), 3917–3929.
Ivkovic, D., Markovic, M., Todorovic, B.S., Balestra, C., Marroni, A., Zarkovic, M., 2015. Energetic, exergetic and economic assessment of oxygen production from two columns cryogenic air separation unit. Energy 90 (2), 1298–1316.
Jones, D., Bhattacharyya, D., Turton, R., Zitney, S.E., 2011. Optimal design and integration of an air separation unit (ASU) for an integrated gasification combined cycle (IGCC) power plant with CO 2 capture. Fuel Process. Technol. 92 (9), 1685–1695.
Khan, M.N., Tlili, I., 2018. Innovative thermodynamic parametric investigation of gas and steam bottoming cycles with heat exchanger and heat recovery steam generator: Energy and exergy analysis. Energy Rep. 4, 497–506.
Kim, T., Kim, Y., Kim, S.K., 2011. Numerical study of cryogenic liquid nitrogen jets at supercritical pressures. J. Supercrit. Fluids 56 (2), 152–163.
Lee, J.J., Kim, Y.S., Cha, K.S., Tong, S.K., Sohn, J.L., Yong, J.J., 2009. Influence of system integration options on the performance of an integrated gasification combined cycle power plant. Appl. Energy 86 (9), 1788–1796.
Lee, J.C., Lee, H.H., Yong, J.J., Chang, H.L., Min, O., 2014. Process simulation and thermodynamic analysis of an IGCC (integrated gasification combined cycle) plant with an entrained coal gasifier. Energy 64 (1), 58–68.
Liszka, M., Tuka, J., 2012. Parametric study of GT and ASU integration in case of IGCC with CO2 removal. Energy 45 (1), 151–159.
Obara, S., Morel, J., IOkada, M., Kobayashi, K., 2016. Study on the load following characteristics of a distributed IGCC for independent microgrid. Energy 115, 13–25.
Smith, A.R., Klosek, J., 2001a. A review of air separation technologies and their integration with energy conversion processes. Fuel Process. Technol. 70 (2), 115–134.
Smith, A.R., Klosek, J., 2001b. A review of air separation technologies and their integration with energy conversion processes. Fuel Process. Technol. 70 (2), 115–134.
Tang, L., Qu, J., Mi, Z., Bo, X., Chang, X., Anadon, L.D., Wang, S., Xue, X., Li, S., Wang, X., Zhao, X., 2019. Substantial emission reductions from chinese power plants after the introduction of ultra-low emissions standards. Nat. Energy.
Wang, M., Liu, G., Hui, C.W., 2016. Simultaneous optimization and integration of gas turbine and air separation unit in IGCC plant. Energy 116, 1294–1301.
Wang, M., Oyedun, A., Pahija, E., Zhu, Y., Liu, G., Hui, D., 2015. Integration and optimization of an air separation unit (ASU) in an IGCC plant. Comput. Aided Chem. Eng. 37, 509–514.
Xu, J., Wang, T., Chen, Q., Zhang, S., Tan, J., 2019a. Performance design of a cryogenic air separation unit for variable working conditions using the lumped parameter model. Front. Mech. Eng..
Xu, J., Wang, K., Sheng, H., Gao, M., Zhang, S., Tan, J., 2019b. Energy efficiency optimization for ecological 3D printing based on adaptive multi-layer customization. J. Cleaner Prod. 245.
Zang, G., Tejasvi, S., Ratner, A., Lora, E.S., 2018. A comparative study of biomass integrated gasification combined cycle power systems: Performance analysis. Bioresour. Technol. 255, 246–256.
Zhang, J., Zhou, Z., Ma, L., Li, Z., Ni, W., 2013. Efficiency of wet feed IGCC (integrated gasification combined cycle) systems with coal water slurry preheating vaporization technology. Energy 51, 137–145.

Jinghua Xu, born in 1979, is currently an associate professor at *Zhejiang University, China*. He received his Ph.D. from *Zhejiang University, China*, in 2009. His research interests include mechanical design. Email: xujh@zju.edu.cn

Tiantian Wang, born in 1995, is currently a Master Degree Candidate in mechanical engineering college, *Zhejiang University, China*. His research interests include CAD. Email: 21725118@zju.edu.cn

Mingyu Gao, born in 1996, is currently a Master Degree Candidate in mechanical engineering college, *Zhejiang University, China*. His research interests include deep learning. E-mail: 3140104348@zju.edu.cn

Tao Peng, born in 1987, is currently a branch manager in Hangzhou Turbine Machinery Equipment CO. LTD, China. His research interests include energy conservation and pollution emissions reduction. E-mail: pengtao@htc.net.cn

Shuyou Zhang, born in 1963, is currently a professor at *Zhejiang University, China*. He received his Ph.D. from *Zhejiang University, China*, in 1999. His research interests include CAD/CG. E-mail: zsy@zju.edu.cn

Jianrong Tan, born in 1954, is currently an academician of Chinese Academy of Engineering and a professor of mechanical engineering college, Zhejiang University, China. He received his Ph.D. from *Zhejiang University, China*, in 1992. His research interests include product design methodology. E-mail: egi@zju.edu.cn